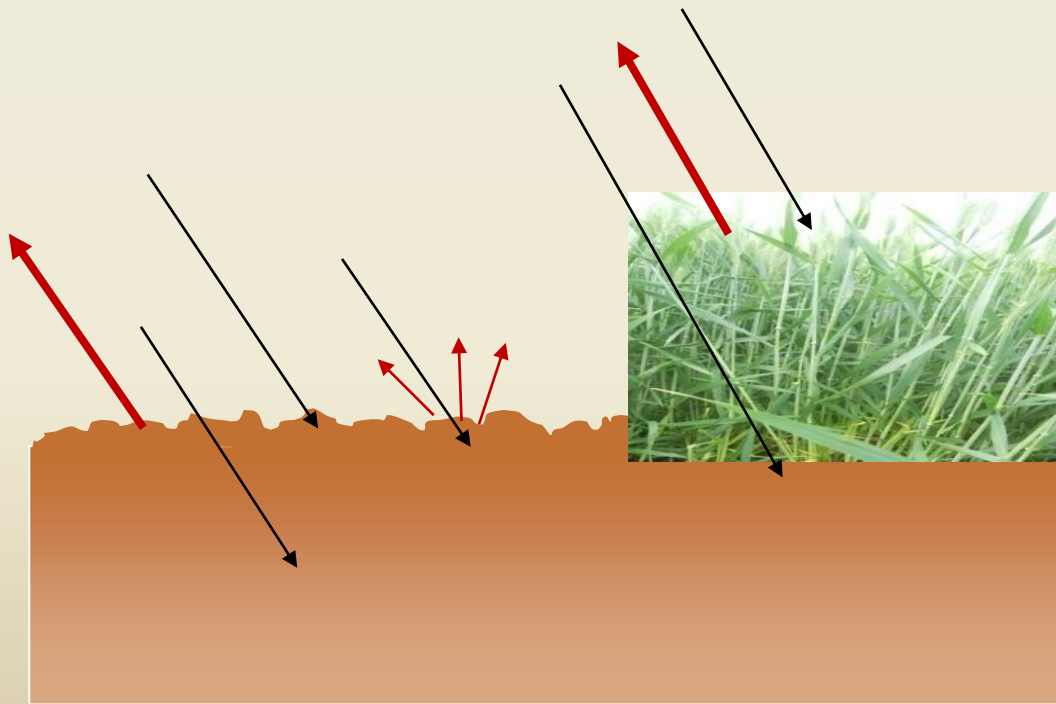
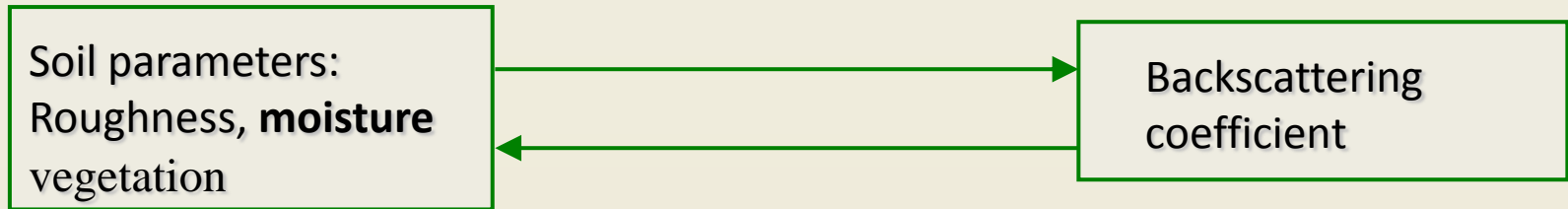


Effet de la rugosité des surfaces continentales sur la mesure radar

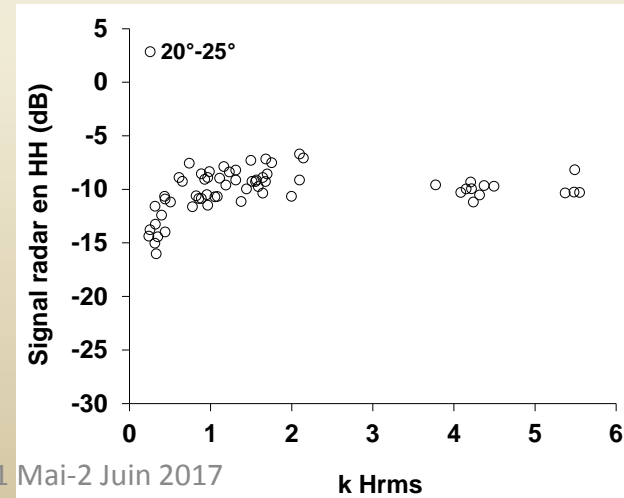
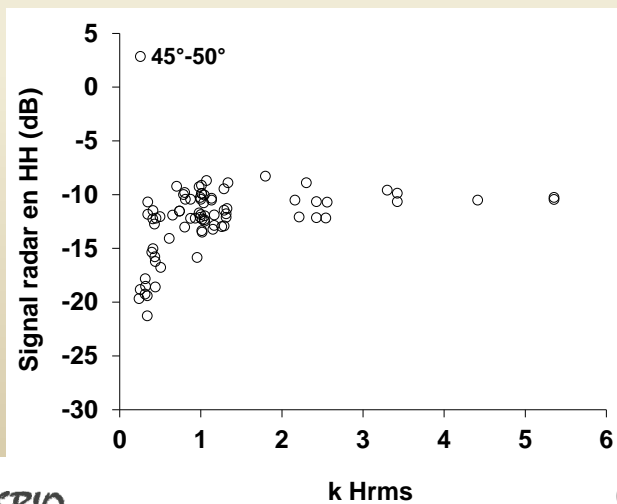
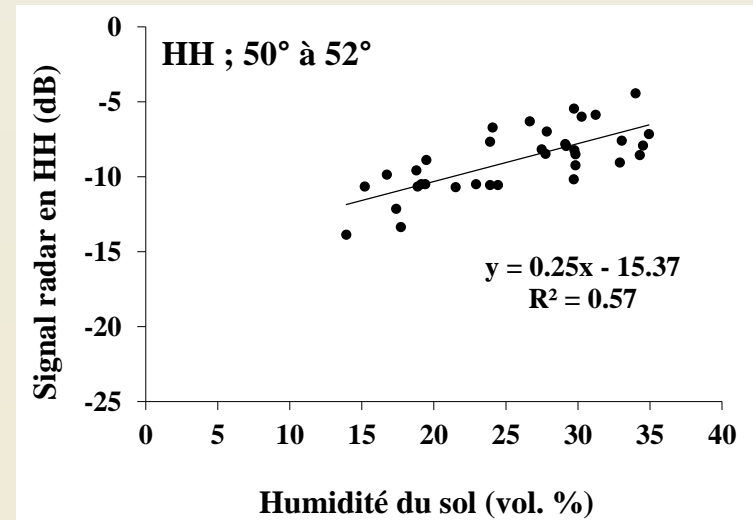
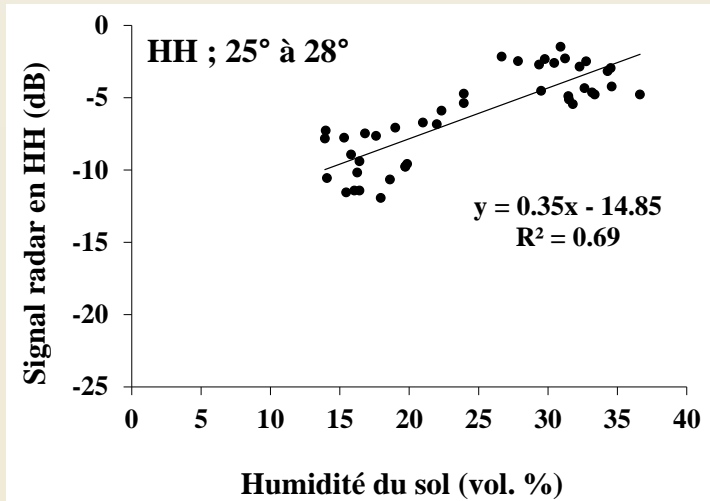
M. Zribi, N. Baghdadi



INTRODUCTION



RADAR SIGNAL SENSITIVITY TO SURFACE PARAMETERS

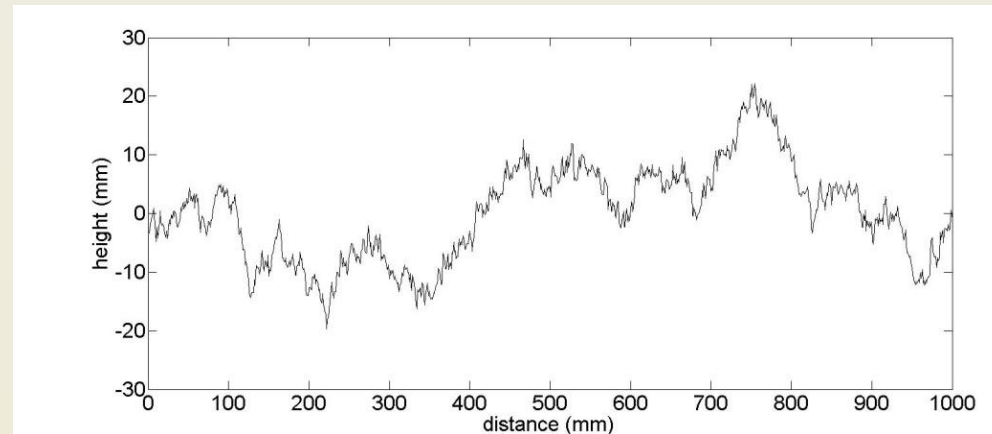


$$\rho(x) = Hrms^2 \exp\left(-\left(\frac{x}{L}\right)^\alpha\right)$$

Hrms: Rms height

L: Correlation length

α : power of height correlation function



References	New descriptions or improvements
Shi et al., 1997	General power law Spectrum
Rouvier et al., 2000 Zribi et al., 2000	Fractal brownian approach, introduction of fractal dimension D
Mattia et al. 1997, Davidson et al. 2000, Oh et al., 1998 Zribi et al., 2000	Statistics, length of the profile Introduction of fractal structures in correlation function shape
Li et al, 02, Fung, 1994, Zribi et al., 2005	Analysis of correlation function shape
Lievens et al., 2011	Effective roughness parameter
Baghdadi et al. 2006, 2011, 2012	Fitting parameter $L_{opt}=f(Hrms)$

→ C and X bands

- Proposition of new Z_g parameter
- Validation with experimental campaigns

→ P band

- Roughness multi-scale analysis
- Validation with experimental campaigns

Numerical backscattering modelling: Surface profile generation



$$\rho(x) = s2 \exp\left(-\left(\frac{x}{l}\right)^\alpha\right)$$

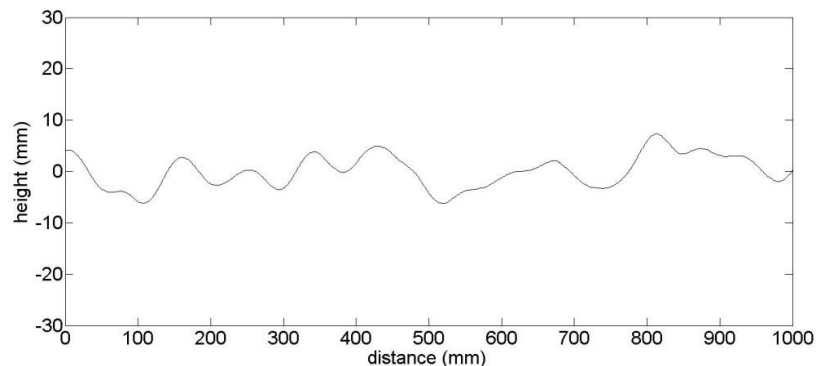
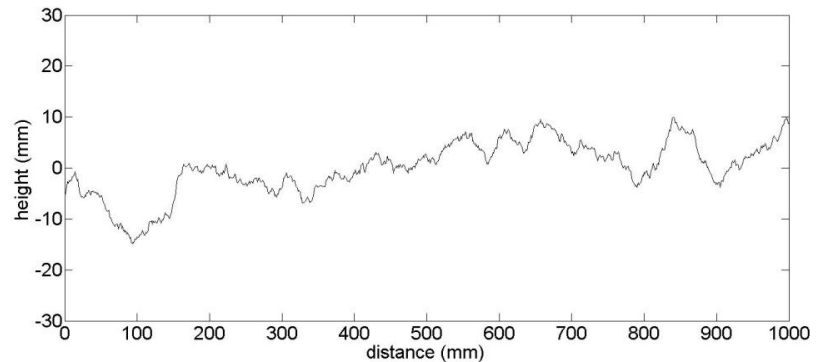
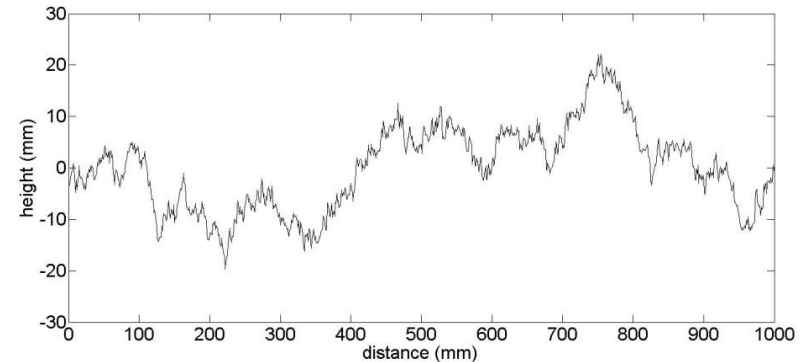
s : Rms height

l : Correlation length

$$h(k) = \sum_{i=-M}^{i=M} W(i)X(i+k)$$

$$W(i) = F^{-1}\left[\sqrt{F[C(i)]}\right]$$

Three synthetically generated surface profiles, with rms height=0.6 cm, correlation length=6 cm, and a) $\alpha=1$, b) $\alpha=1.5$ and c) $\alpha=2$.



$$\left\{ \begin{array}{l} \vec{n} \times \vec{E}^i(\vec{r}) = -\frac{1}{2} \vec{K} + \vec{n} \times \int_c \left[j\omega\mu_0 G_1 \vec{J} - \vec{K} \times \nabla G_1 - \frac{\nabla' \cdot \vec{J}}{j\omega\epsilon_1} \nabla G_1 \right] dl' \\ \vec{n} \times \vec{H}^i(\vec{r}) = -\frac{1}{2} \vec{J} + \vec{n} \times \int_c \left[j\omega\epsilon_1 G_1 \vec{K} + \vec{J} \times \nabla G_1 - \frac{\nabla' \cdot \vec{K}}{j\omega\mu_0} \nabla G_1 \right] dl' \\ 0 = -\frac{1}{2} \vec{K} - \vec{n} \times \int_c \left[j\omega\mu_0 G_2 \vec{J} - \vec{K} \times \nabla G_2 - \frac{\nabla' \cdot \vec{K}}{j\omega\epsilon_2} \nabla G_2 \right] dl' \\ 0 = -\frac{1}{2} \vec{J} - \vec{n} \times \int_c \left[j\omega\epsilon_0 G_2 \vec{K} + \vec{J} \times \nabla G_2 - \frac{\nabla' \cdot \vec{K}}{j\omega\epsilon_2} \nabla G_2 \right] dl' \end{array} \right.$$

$$G_i = -\frac{j}{4} H_0^{(2)}(k_i |\vec{\rho} - \vec{\rho}'|), i = 1, 2$$

$$\begin{cases} E_y^i(\vec{\rho}) = \frac{1}{2} E_y(\vec{\rho}) + \int_c \left[j\omega\mu_0 G_1 J_y + E_y(\vec{n}' \cdot \nabla G_1) \right] dl' \\ 0 = \frac{1}{2} E_y(\vec{\rho}) - \int_c \left[j\omega\mu_0 G_2 J_y + E_y(\vec{n}' \cdot \nabla G_2) \right] dl' \end{cases}$$

$$\begin{bmatrix} Q^{11} & Q^{12} \\ Q^{21} & Q^{22} \end{bmatrix} \begin{bmatrix} E_y \\ J_y \end{bmatrix} = \begin{bmatrix} E_y^i \\ 0 \end{bmatrix}$$

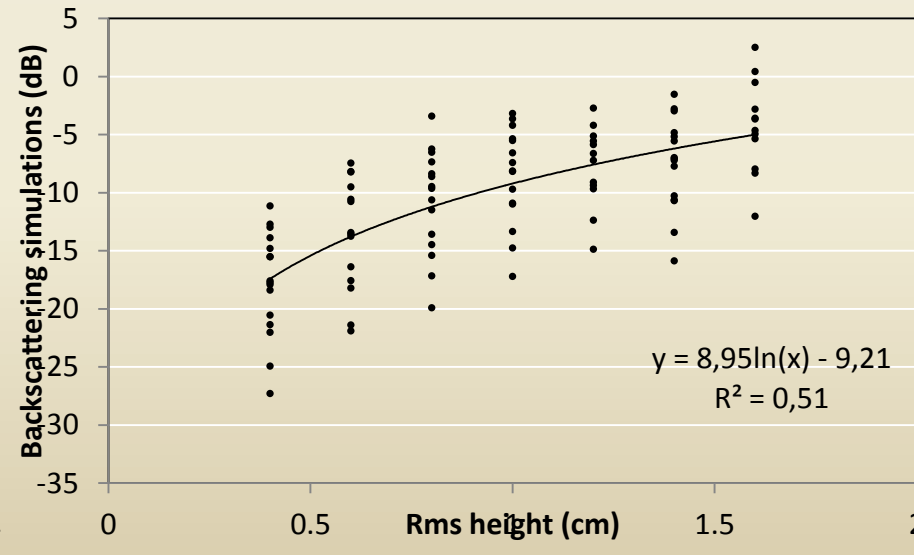
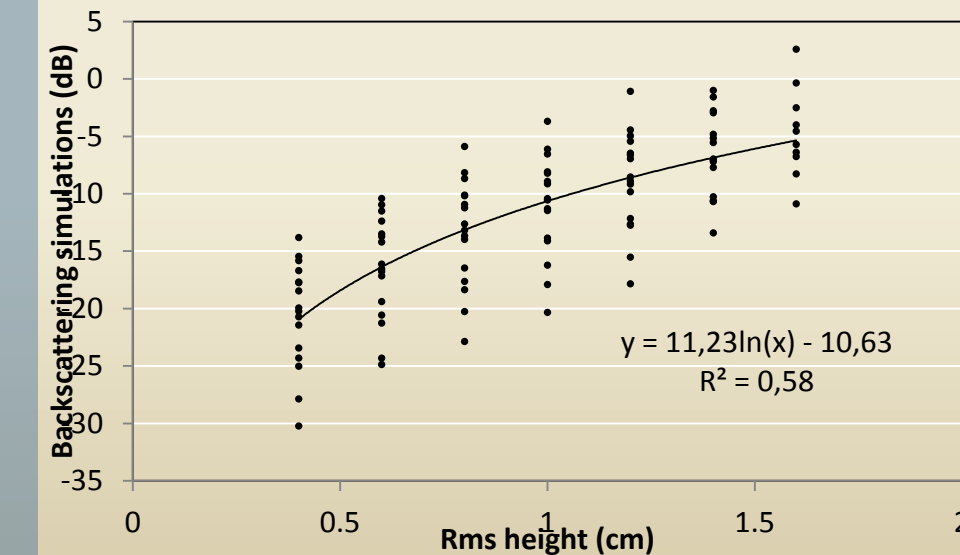
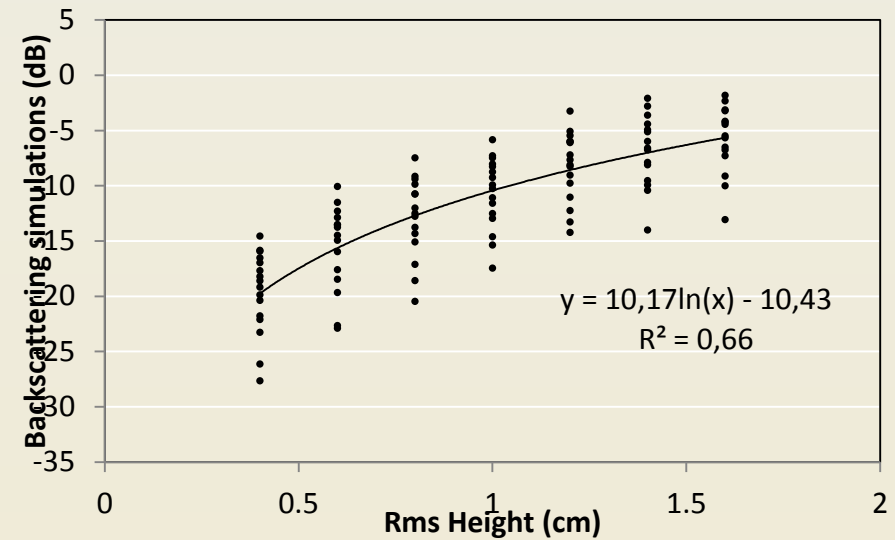
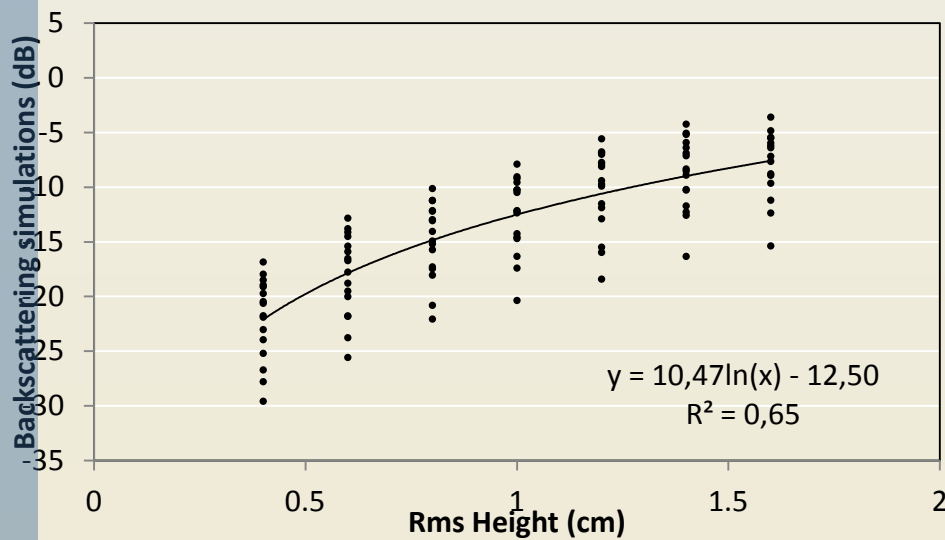
$$E_y^s = - \int_c \left[j\omega\mu_0 G_1 J_y + E_y(\vec{n}' \cdot \nabla G_1) \right] dl'$$

$$\sigma^0 = \frac{2\pi\rho}{PL_{eff}} \left[\sum_{j=1}^P |E_j^s|^2 - \frac{1}{P} \left| \sum_{j=1}^P E_j^s \right|^2 \right]$$

Simulations will be proposed for: rms heights $s=0.4$ cm, $s=0.6$ cm, $s=0.8$ cm, $s=1$ cm, $s=1.2$ cm, $s=1.4$ cm, $s=1.6$ cm; correlation lengths $l=4$ cm, $l=6$ cm, $l=8$ cm and $l=10$ cm; a parameter $a=1$, $a=1.25$, $a=1.5$ and $a=1.75$.

HH, VV polarisations, 20 and 40° incidence angles, Mv=10%, 20%, 30%

Relationships between rms height and backscattering simulations

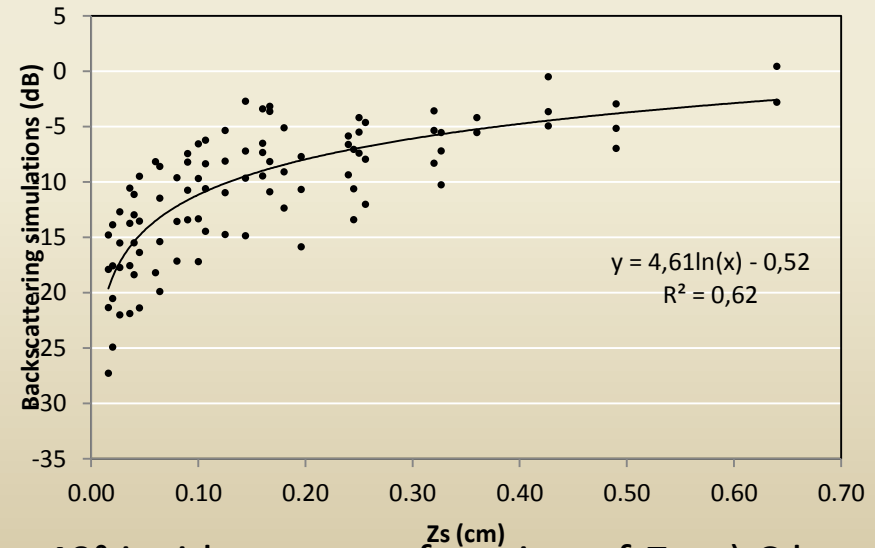
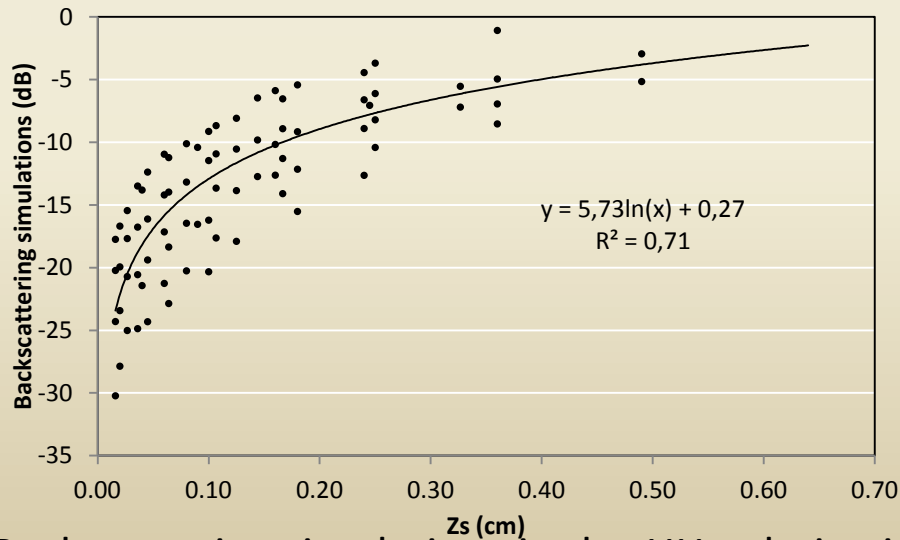
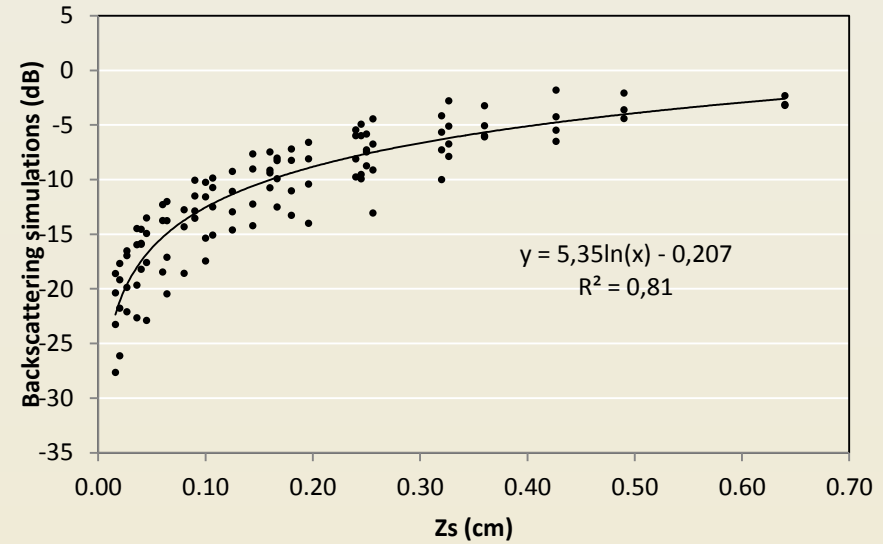
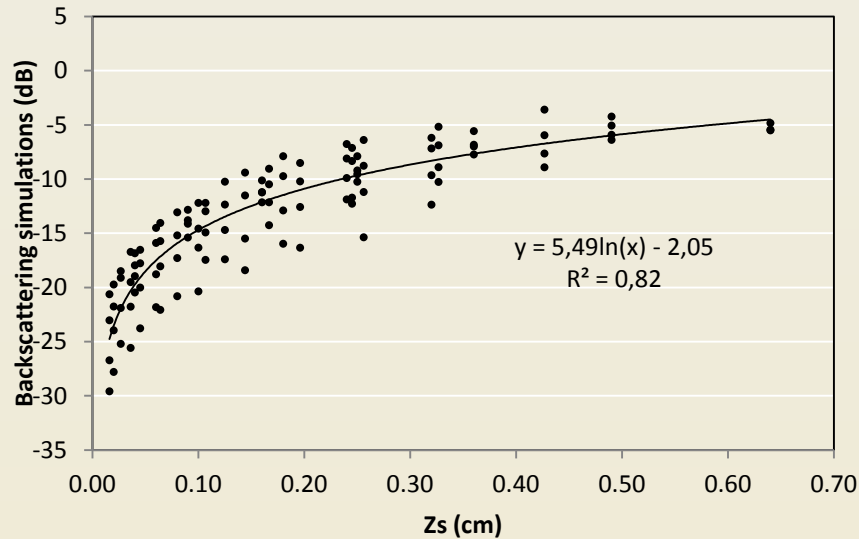


Backscattering simulations in the *HH* polarisation at 40° incidence, as a function of the rms height: a) C band, *mv*=10%, b) C band, *mv*=30%, c) X band, *mv*=10%, d) X band, *mv*=30%

$\sigma = f(Z_s)$



$Z_s = s^2 / l = s \cdot s / l$ (Zribi and Dechambre, 2003)



Backscattering simulations in the *HH* polarisation at 40° incidence, as a function of Z_s . a) C band, $mv=10\%$, b) C band, $mv=30\%$, c) X band, $mv=10\%$, d) X band, $mv=30\%$

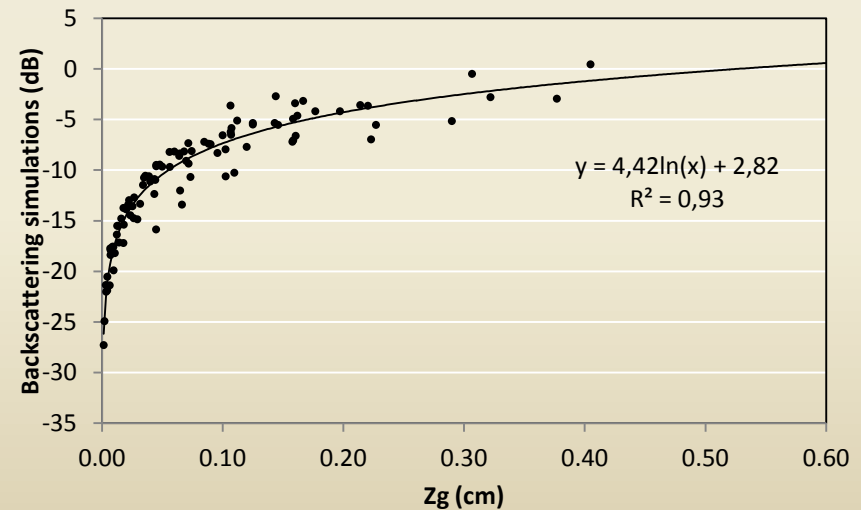
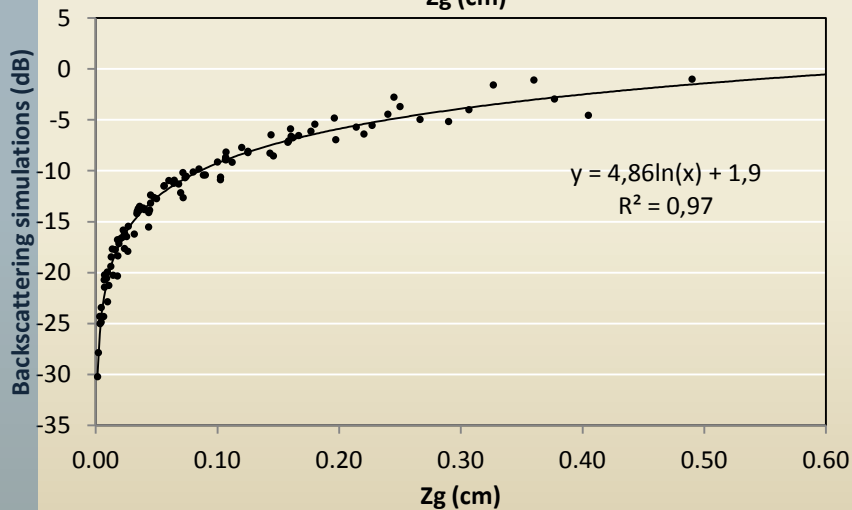
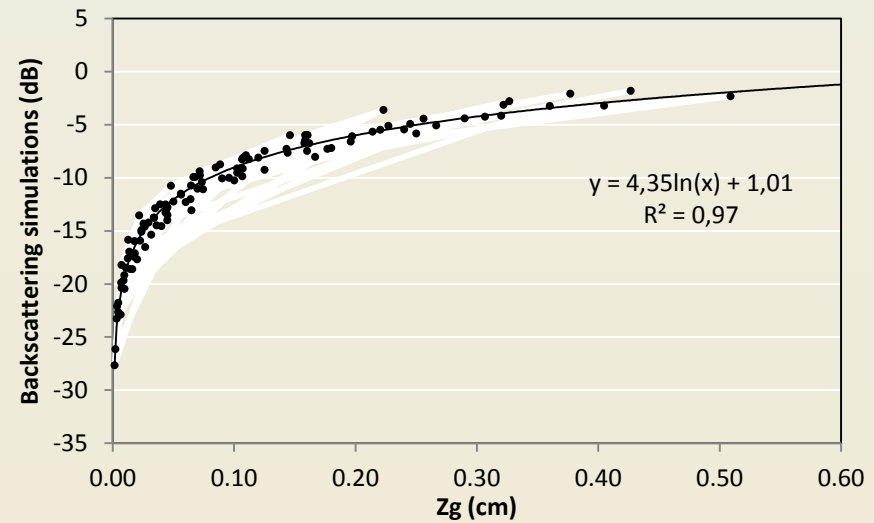
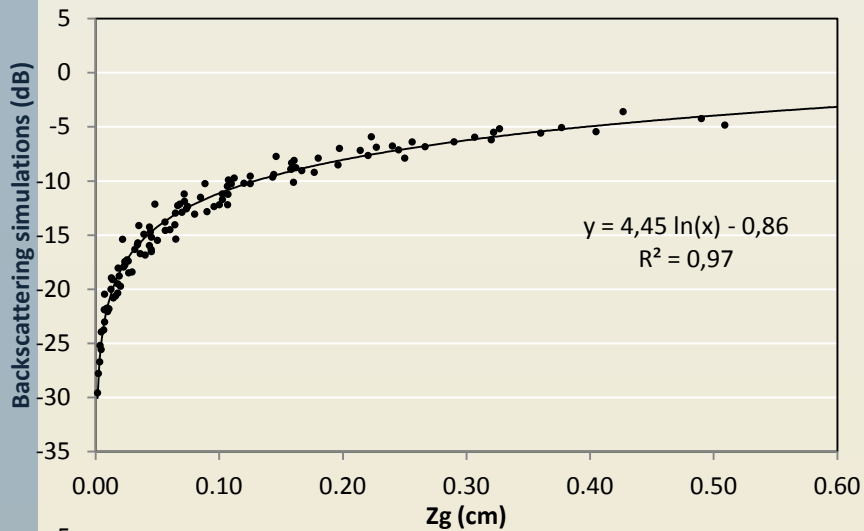
- The parameter Z_s was initially proposed for use with an exponential correlation, and weaker correlations are observed between Z_s and the simulated backscattering when other correlation function shapes are considered.
- Since the contribution of the ratio s/l must be different from one correlation shape to another, we propose to introduce a new parameter, which is a global representation of the Z_s parameter, written as:

$$Z_g = s \cdot \left(\frac{s}{l} \right)^{g(\alpha)}$$

The best correlation between the global roughness parameter Z_g and the simulations was determined by least squares regression.

$$g(\alpha) \approx \alpha \quad \longrightarrow \quad Z_g = s \left(\frac{s}{l} \right)^\alpha$$

Relationships between Z_g and backscattering simulations

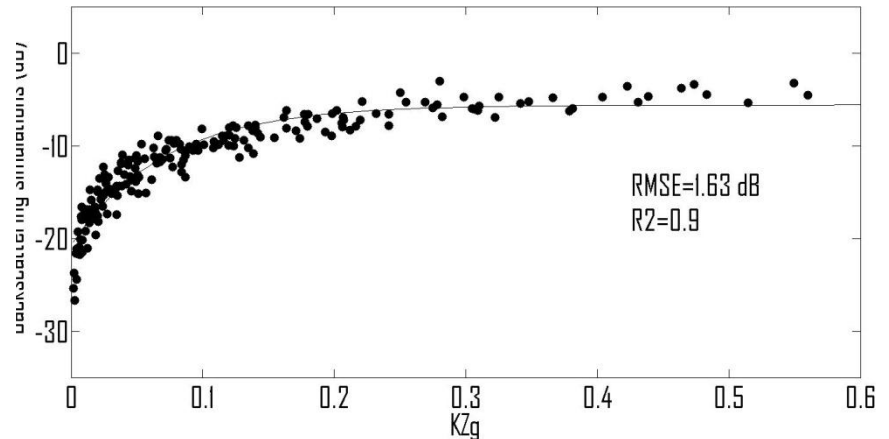
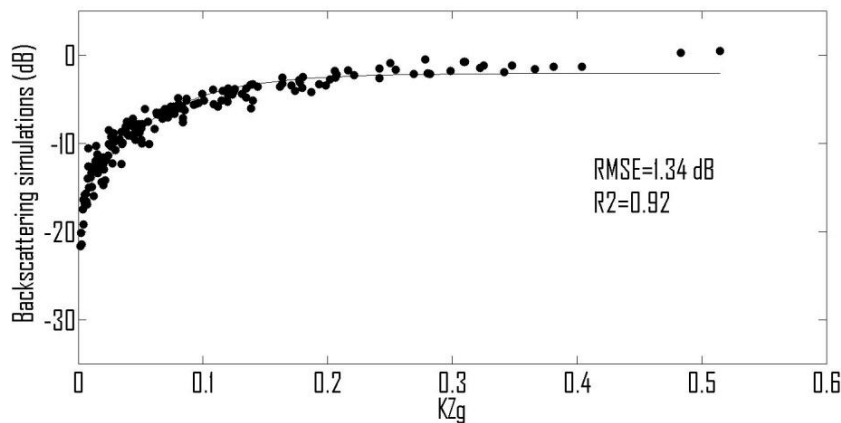
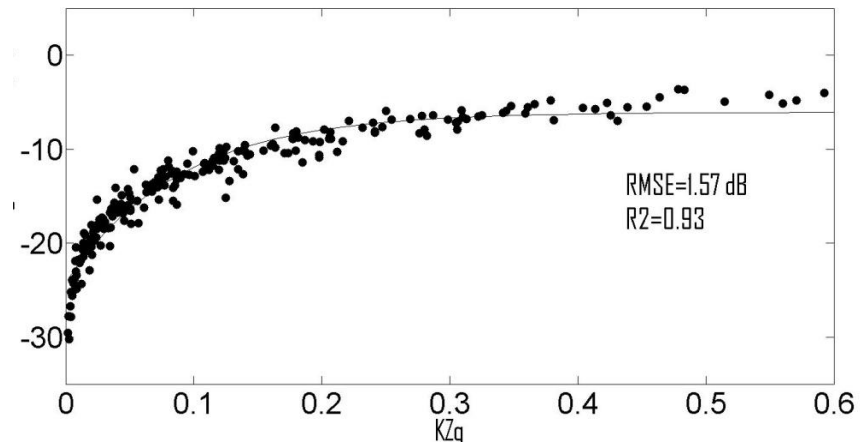
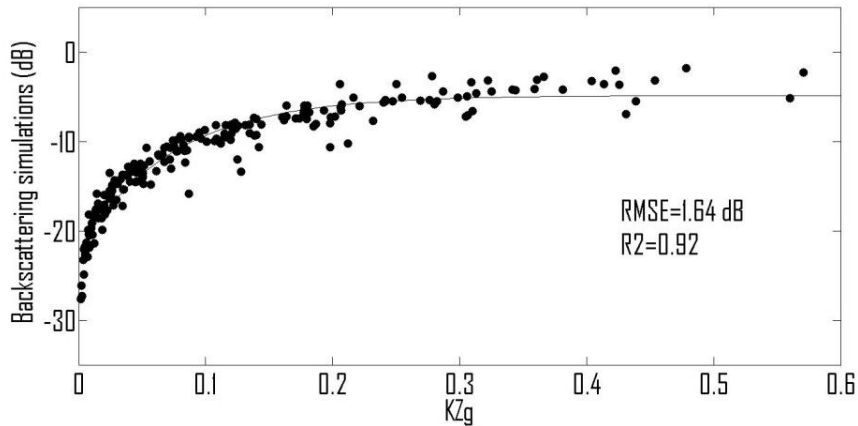


Backscattering simulations in the HH polarisation at 40° incidence as a function of the parameter Z_g , C band, $mv=10\%$, b) C band, $mv=30\%$, c) X band, $mv=10\%$, d) X band, $mv=30\%$

Relationships between kZg and backscattering simulations (C & X bands)



$$\sigma^0 = \alpha + \beta(1 - e^{-\mu k Zg})$$



Backscattering simulations as a function of the parameter kZg , at 40° : a) *HH* pol, $mv=10\%$, b) *HH* pol, $mv=30\%$, c) *VV* pol, $mv=10\%$, d) *VV* pol, $mv=30\%$

Parameters and correlation coefficients for relationships between KZg and simulations



Configuration		α	β	μ	R^2	RMSE (dB)
M _v =10%	HH-20°	-16.14	12.34	23.71	0.86	1.44
	VV-20°	-15.11	10.21	38.31	0.77	1.53
	HH-40°	-24.19	18.13	11.27	0.93	1.57
	VV-40°	-20.71	15.10	14.02	0.90	1.63
M _v =20%	HH-20°	-14.15	12.11	22.81	0.88	1.37
	VV-20°	-12.54	10.68	33.41	0.84	1.31
	HH-40°	-22.57	17.87	11.28	0.92	1.66
	VV-40°	-21.04	15.46	15.48	0.89	1.72
M _v =30%	HH-20°	-13.05	12.01	22.95	0.87	1.35
	VV-20°	-11.09	10.86	32.26	0.86	1.24
	HH-40°	-22	-17.21	13.43	0.92	1.64
	VV-40°	-17.01	-14.92	17.65	0.92	1.34



Campaign	Sensor	date	Configuration
Orgeval '94	SIRC	12/04/94 - 18/04/94	C band, HH, 44°
Pays de Caux '94	ERASME	February 1994	C and X bands, HH, VV 20°, 25°, 30°, 35°
Villamblain '03	ASAR/ENVISAT	October 2003	C band, HH, ~43°

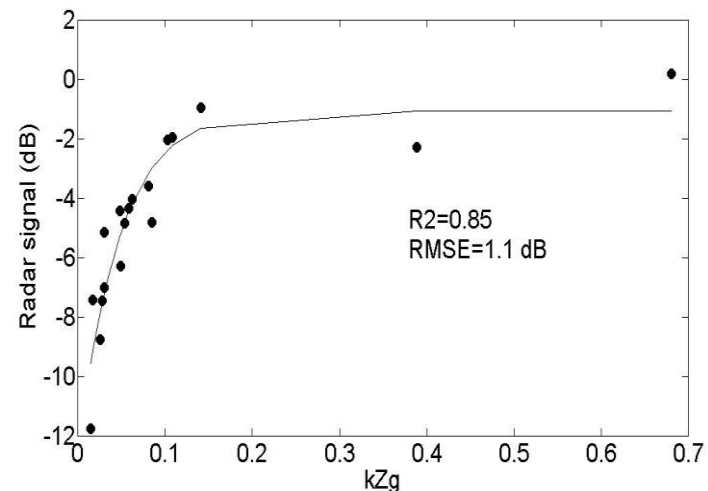
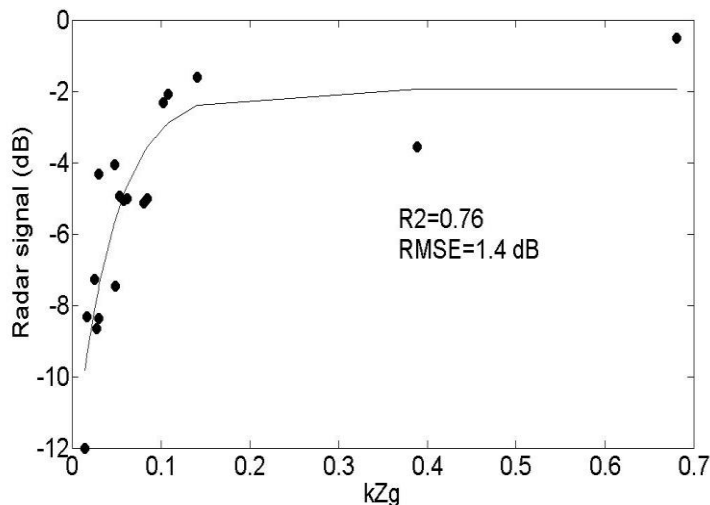
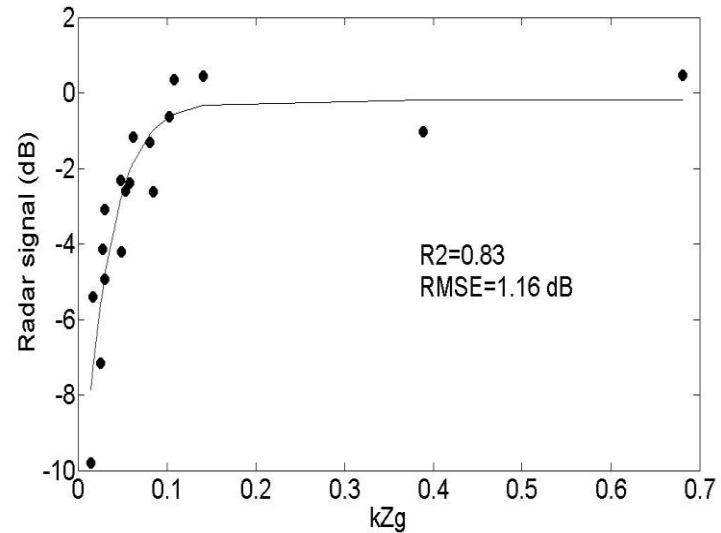
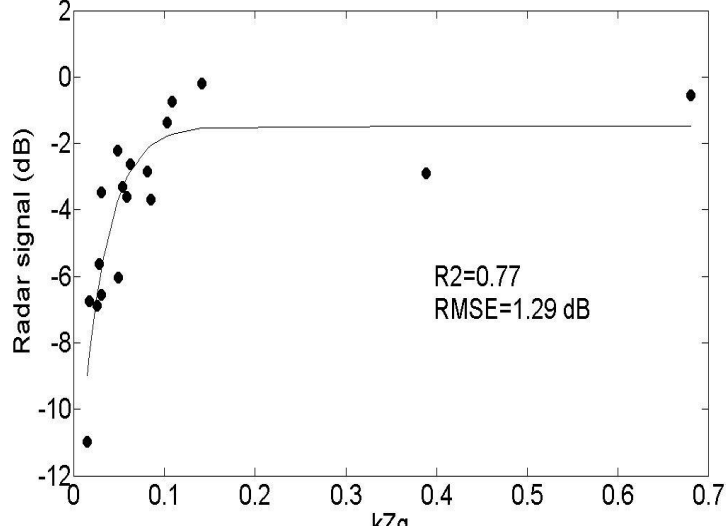
Ground measurements over test fields:

- Roughness (pin-profiler)
- Moisture (gravimetric method or TDR probe)

Relationships between KZg and measured radar data

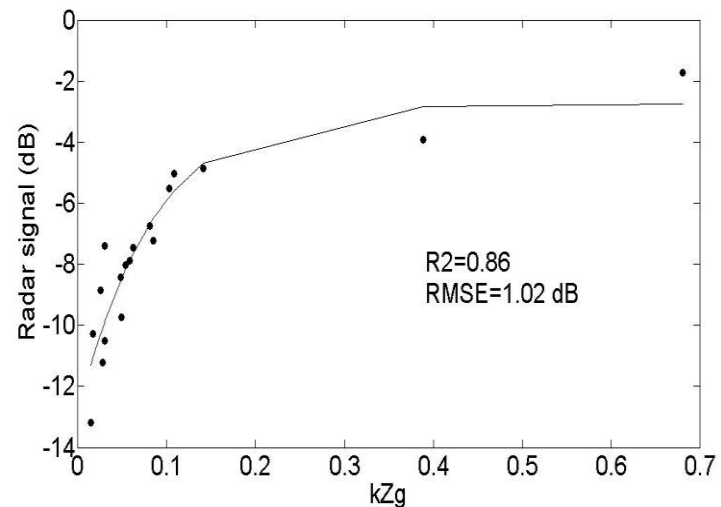
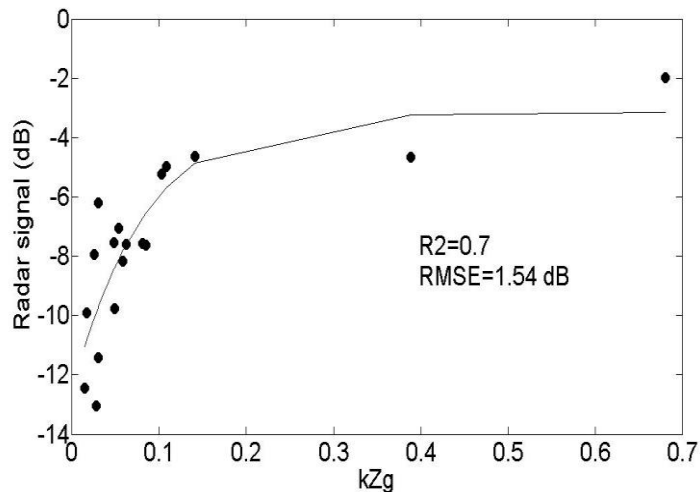
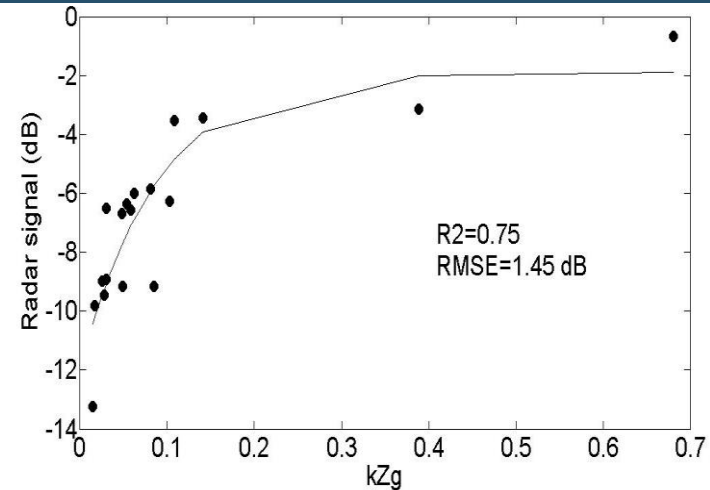
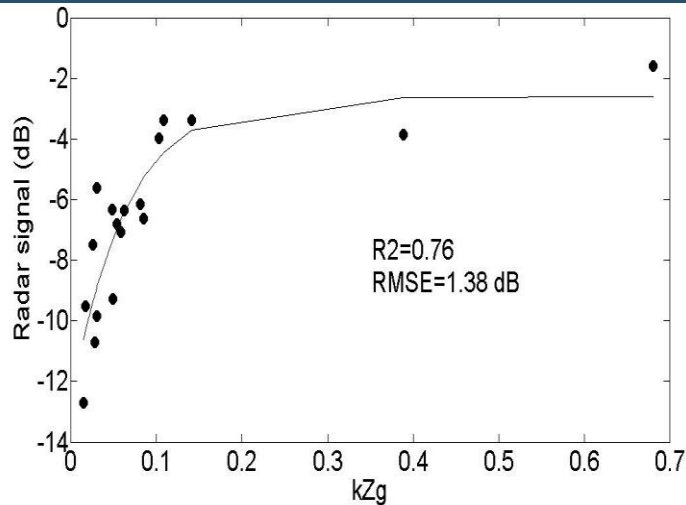


$$\sigma_{p\theta}^0 = \alpha_{p\theta} + \beta_{p\theta} \left(1 - e^{-\mu_{p\theta} k Zg}\right)$$



Relationship between kZg and measured radar signals, for: a) HH pol at 20° , b) VV pol at 20° , c) HH pol at 25° , d) VV pol at 25°

Relationships between kZg and measured radar data

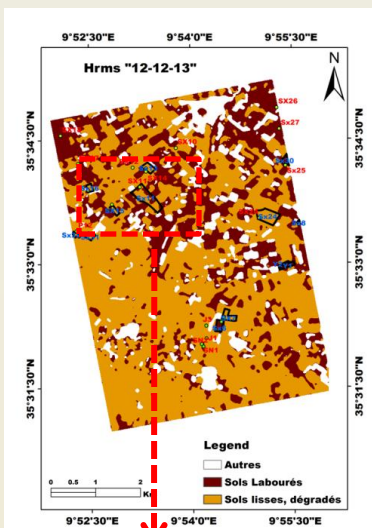
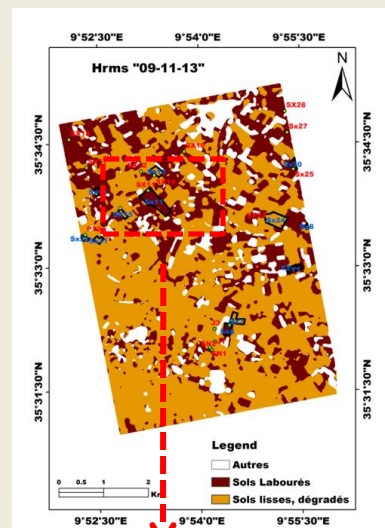


Relationship between kZg and measured radar signals, for: a) HH pol at 30° , b) VV pol at 30° , c) HH pol at 35° , d) VV pol at 35°

SOIL ROUGHNESS MAPPING

Gorrab et al., 2016

Soil roughness mapping (TERRASAR-X
data



09/11/13



12/12/13



09/11/13



12/12/13

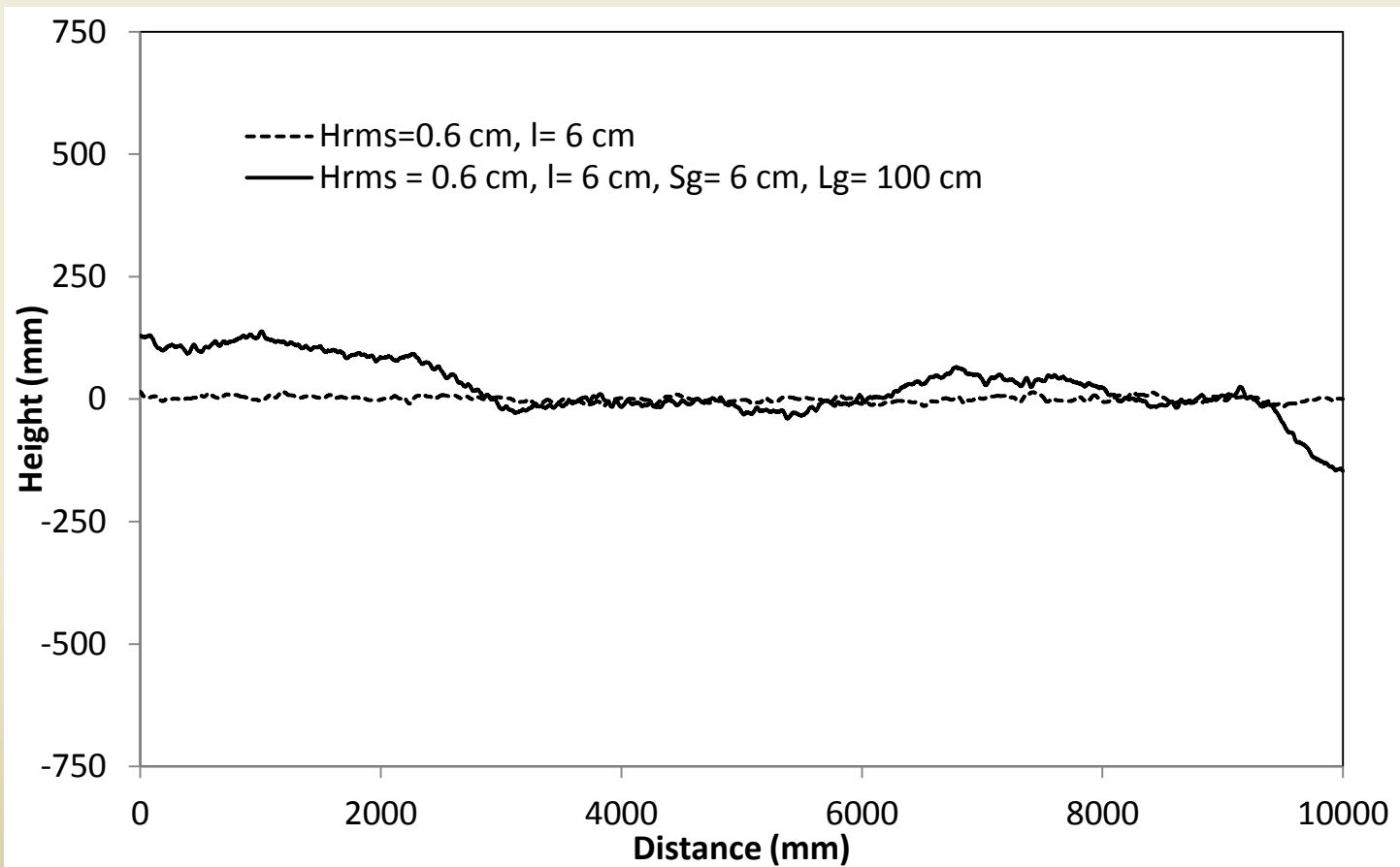
sx11



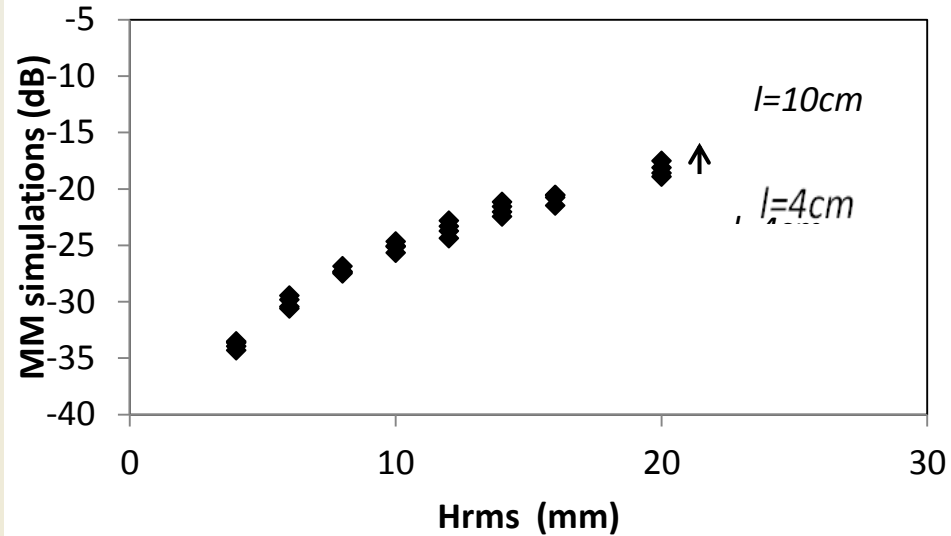
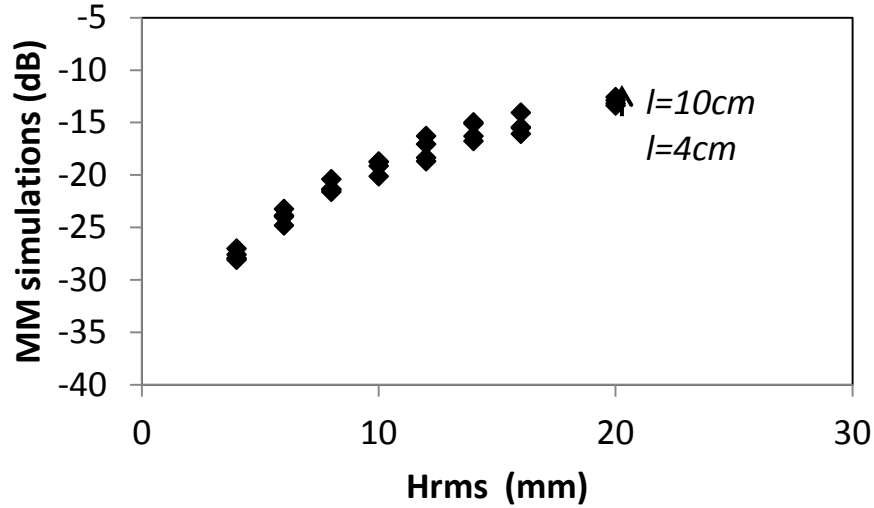
P band?

Multi-scale roughness

$$\rho(x) = H_{rms}^2 \exp\left(-\frac{x}{l}\right) + S_g^2 \exp\left(-\frac{x}{L_g}\right)$$



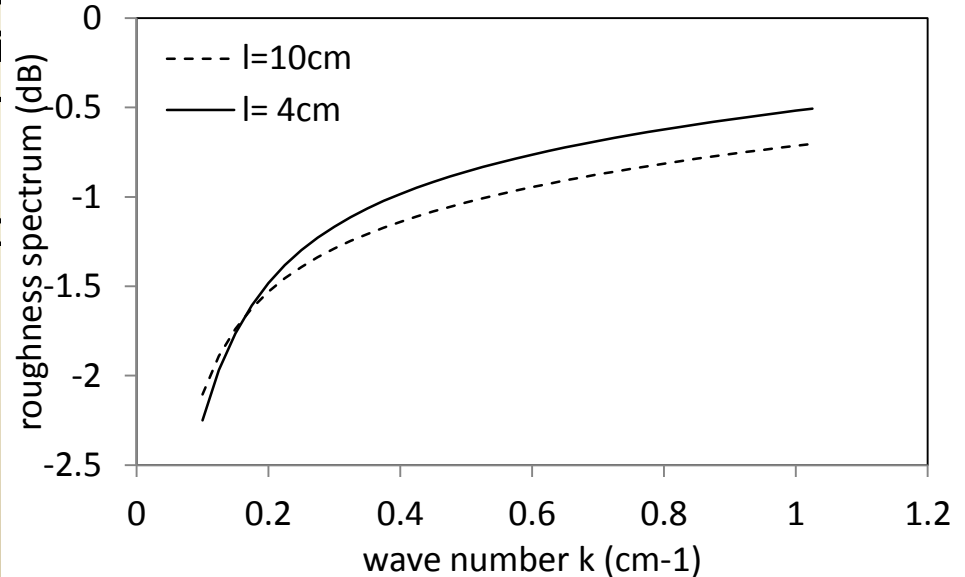
Small scale roughness



Backscattering simulations as a function of surface roughness corresponding to microtopography ($Hrms$) with correlations are made at a 20° and 40° incidence angles.

$Hrms$ effect is dominant, less than l .

$$W = \frac{k^4 l^2 Hrms^2}{(1 + (2kl \sin \theta)^2)^{1.5}}$$

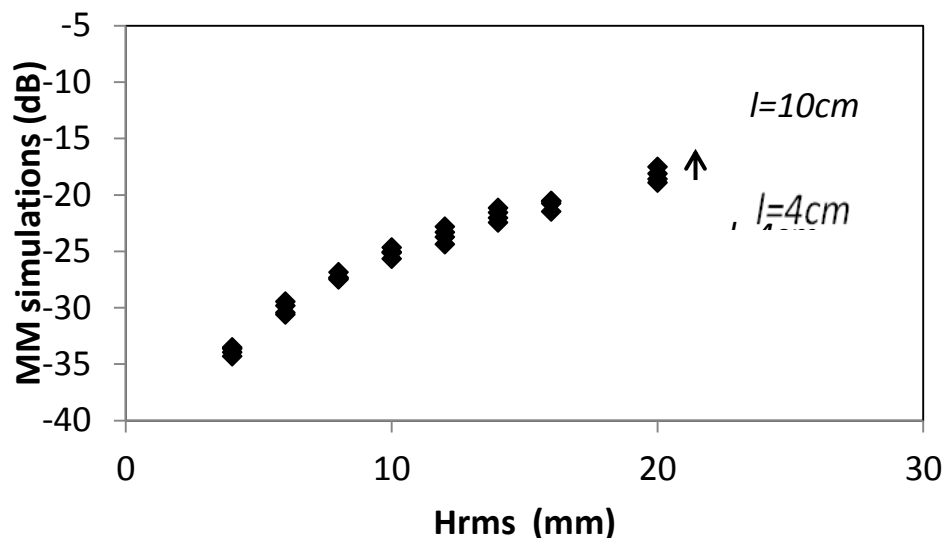
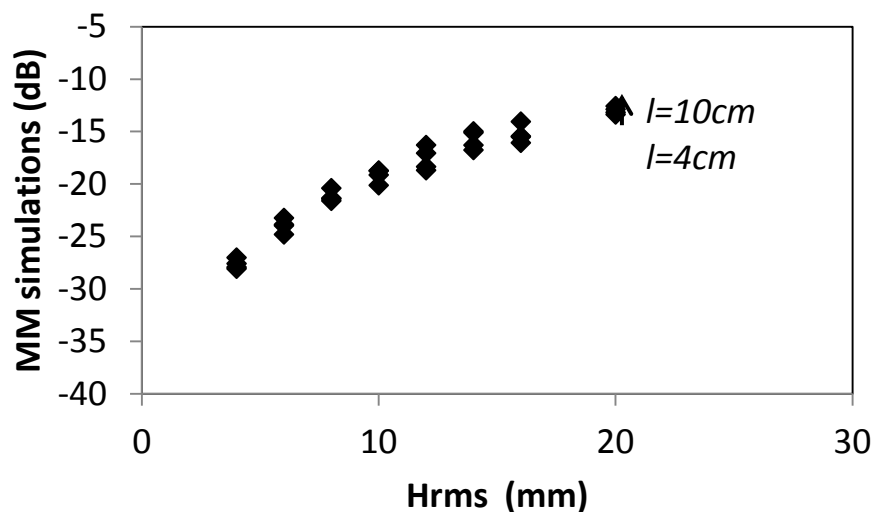


relations

Exponential roughness spectrum as a function of wave number



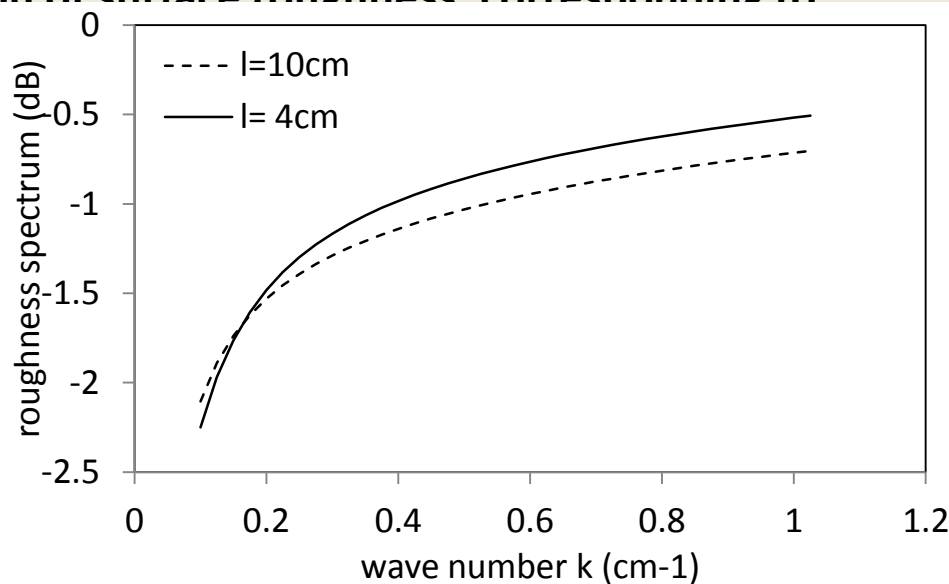
Small scale roughness



Backscattering simulations as a function of surface roughness corresponding to microtopography (*Hrms*) with correlations are made at a 20° and 40° incidence angles.

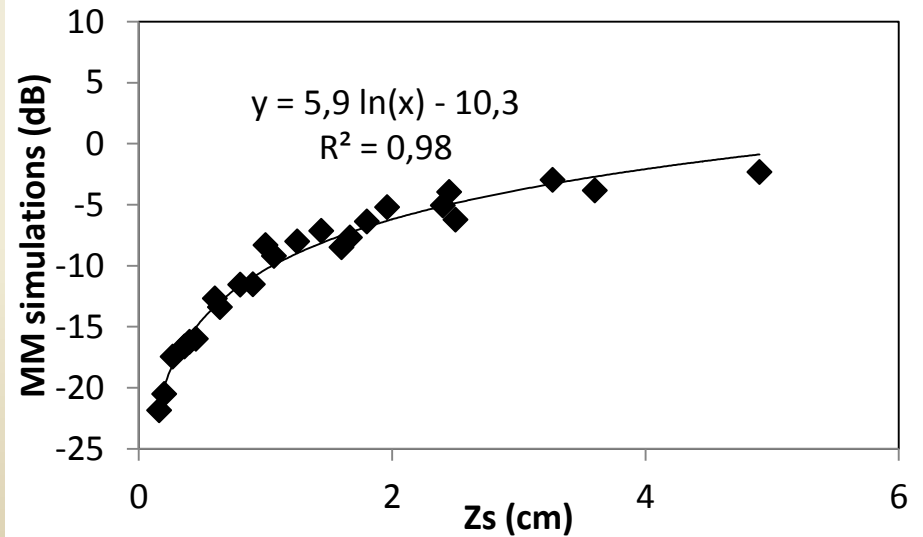
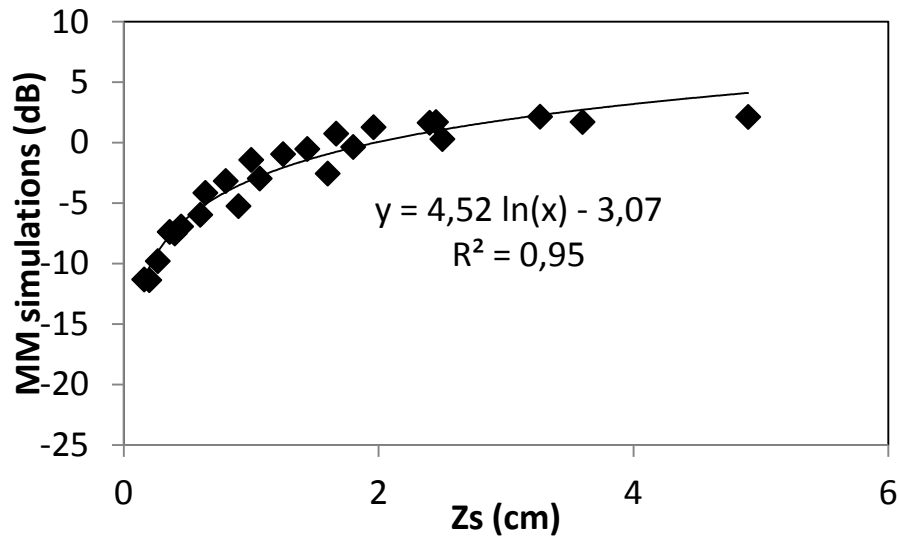
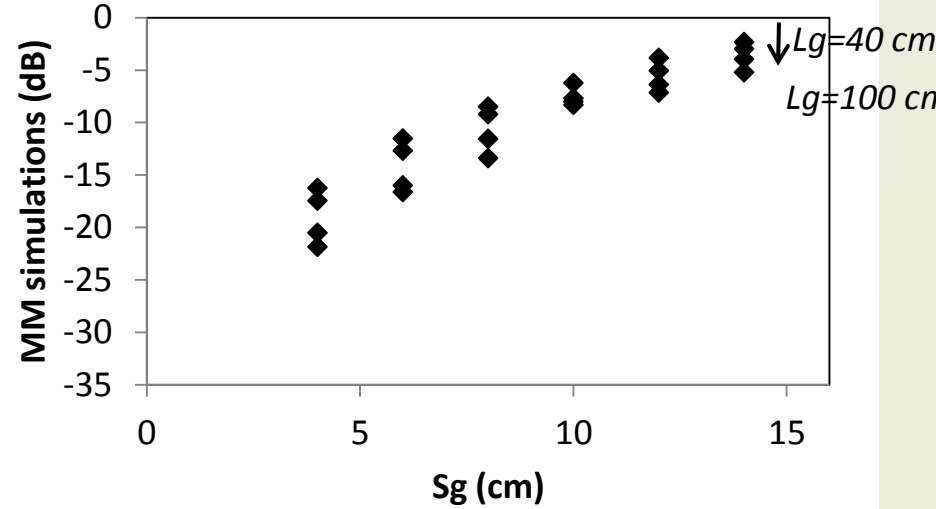
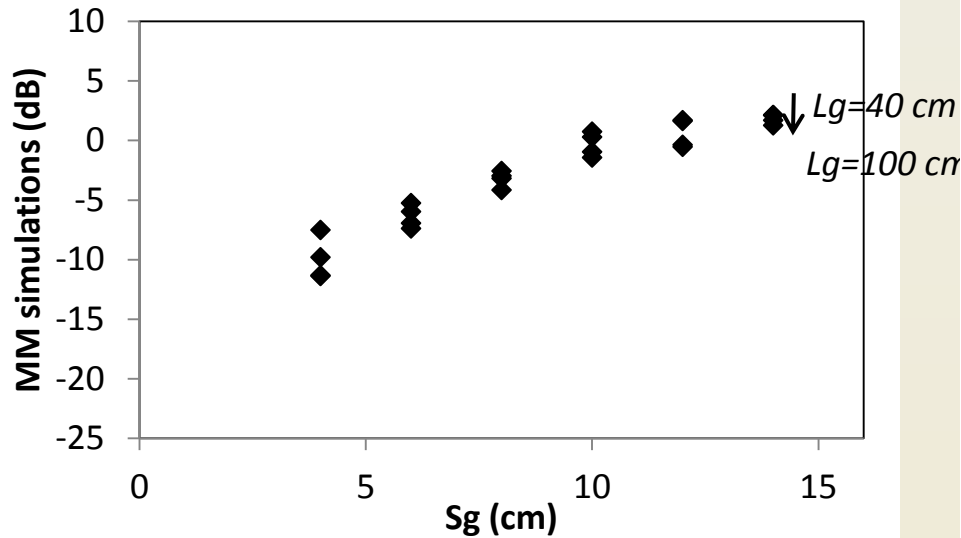
Hrms effect is dominant, less than ...

$$W = \frac{k^4 l^2 Hrms^2}{(1 + (2kl \sin \theta)^2)^{1.5}}$$



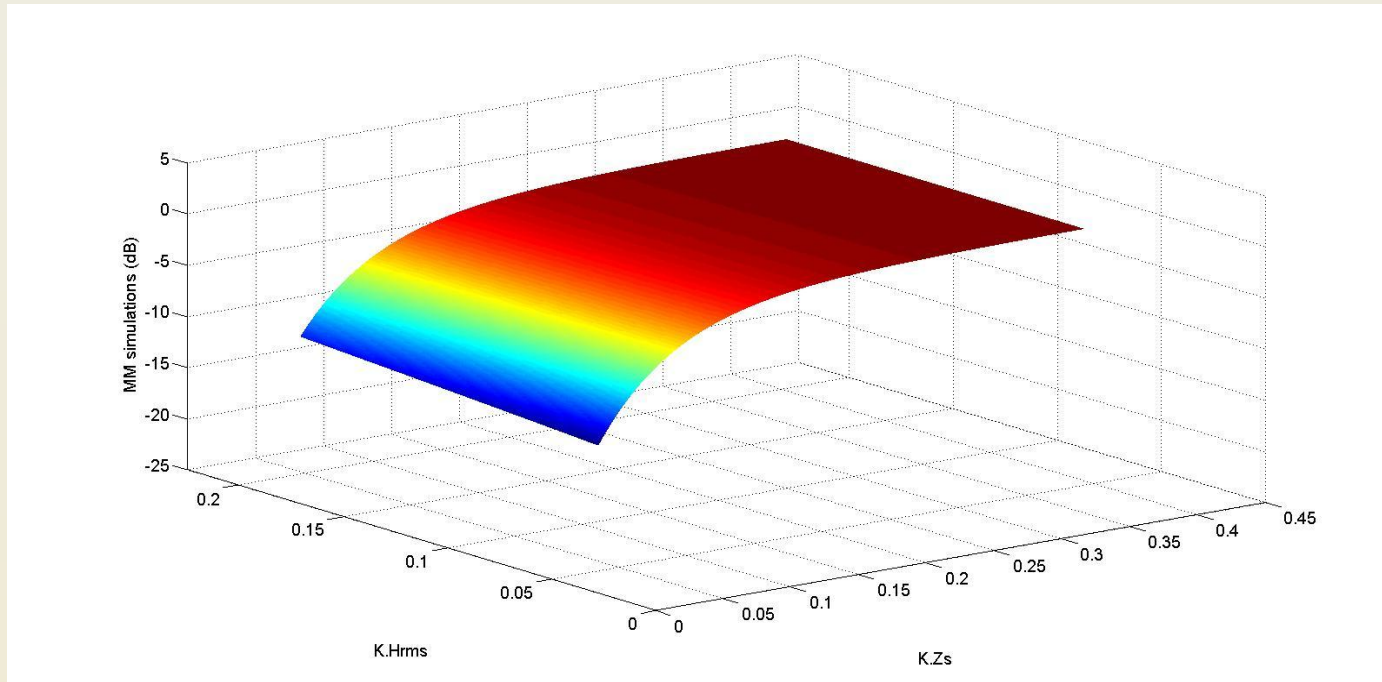
lations

Low roughness structures



Backscattering simulations as a function of surface roughness, corresponding in the case of a low spatial frequency rms height (S_g), with correlation lengths L_g equal to 40, 60, 80 and 100 cm. The simulations are made at a 20° and 40° incidence angles.

MM multiscale simulations



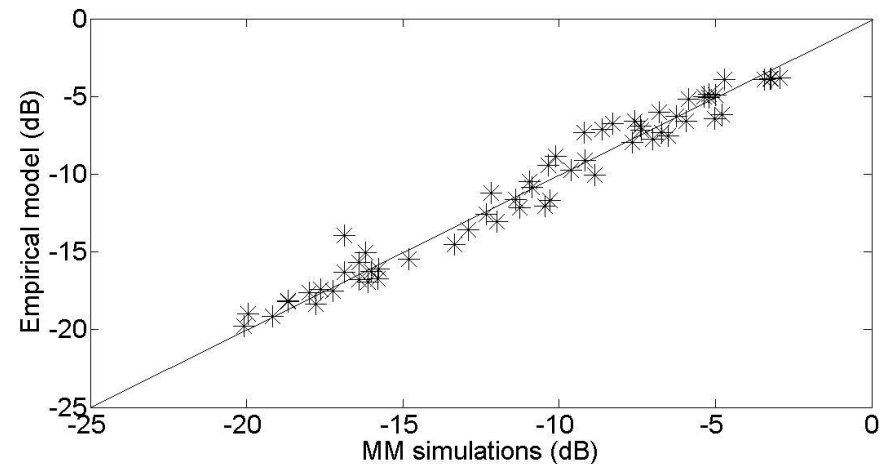
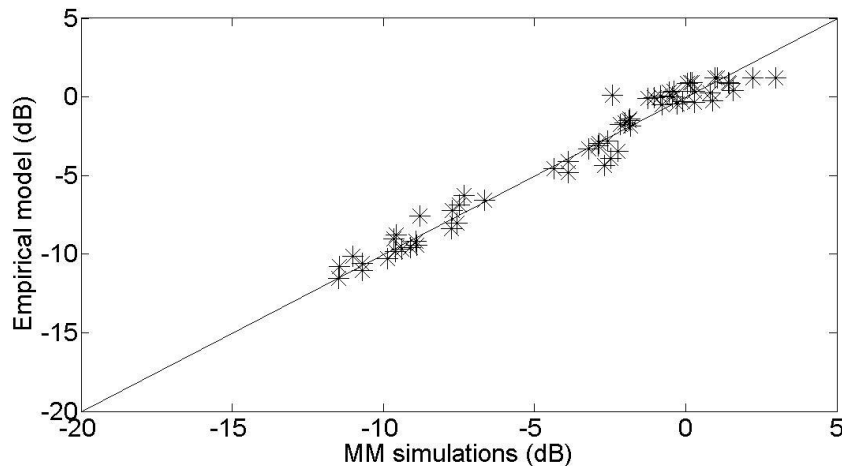
Limited effect of small roughness scale

Roughness spectrum is produced by the sum of two independent exponential spectra corresponding to the small, and to the low spatial frequency, roughness scales described above.

Comparison between MM and empirical simulations

Empirical relationship $\sigma=f(H_{rms}, Z_s)$

$$\sigma^0 = \alpha_{\theta,p} + \beta_{\theta,p} \left(1 - e^{-\left(\mu_{\theta,p} k Z_s + \gamma_{\theta,p} k H_{rms} \right)} \right)$$



The empirical model is validated for all of the roughness conditions analyzed by the moment method simulations, in which $K.H_{rms}$ ranges between 0.036 and 0.18, and $K.Z_s$ ranges between 0.015 and 0.45.

Analysis of real data over agricultural soils

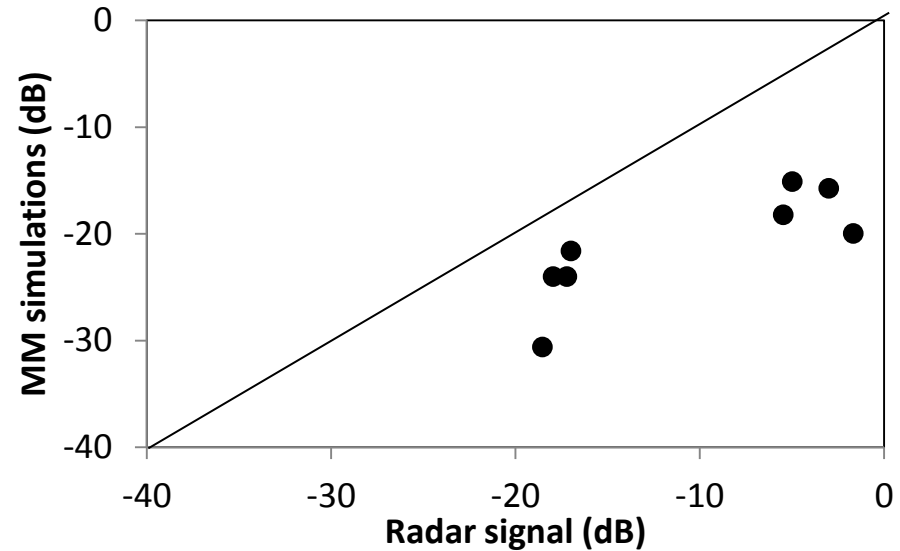
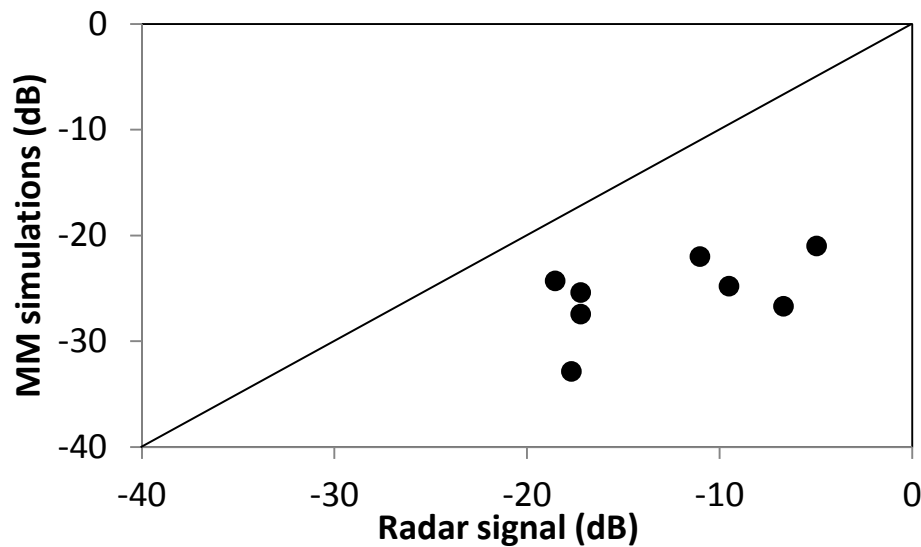
Bordeaux site: this site is located in the southwest of France. The soil is comprised of approximately 19% silt, 29% clay, and 51% sand. On January 21, 2004, fully polarimetric P-band radar data (435 MHz) was acquired by the airborne RAMSES SAR,

Garons site: this site is located near to Nîmes in the South of France. The soil is stony, and is comprised of 54% silt, 40% clay, and 6% sand. Fully polarimetric radar data were acquired in the UHF-band (360 MHz, spatial resolution approximately 0.75 m) on October 4th, 2011,



Study site	Plot number	θ (°)	m_v (vol%)	H_{rms} (cm)	l (cm)
Bordeaux	Bare soil (B1)	53°	26.9	1.89	4.33
	Bare soil (B2)	47°	46.9	0.88	3.22
	Bare soil (B3)	50°	32.9	1.31	3.95
	Bare soil (B4)	52°	39.4	1.69	4.30
Garons	Bare soil (G1)	43°	4	1.56	4.80
	Bare soil (G2)	45°	4.3	1.40	3.34
	Bare soil (G3)	34°	4.4	0.59	3.27
	Bare soil (G4)	46°	2.8	1.25	3.80

Comparison between real radar data and MM simulations

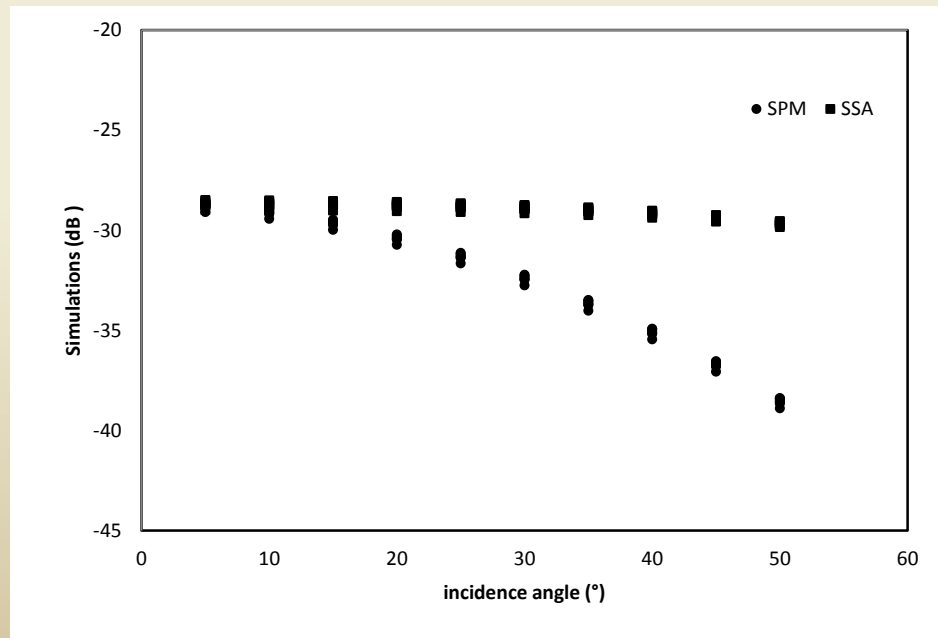
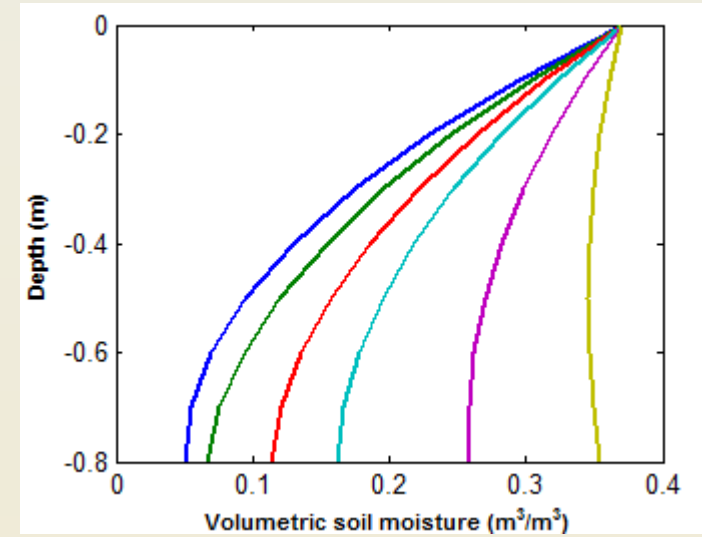
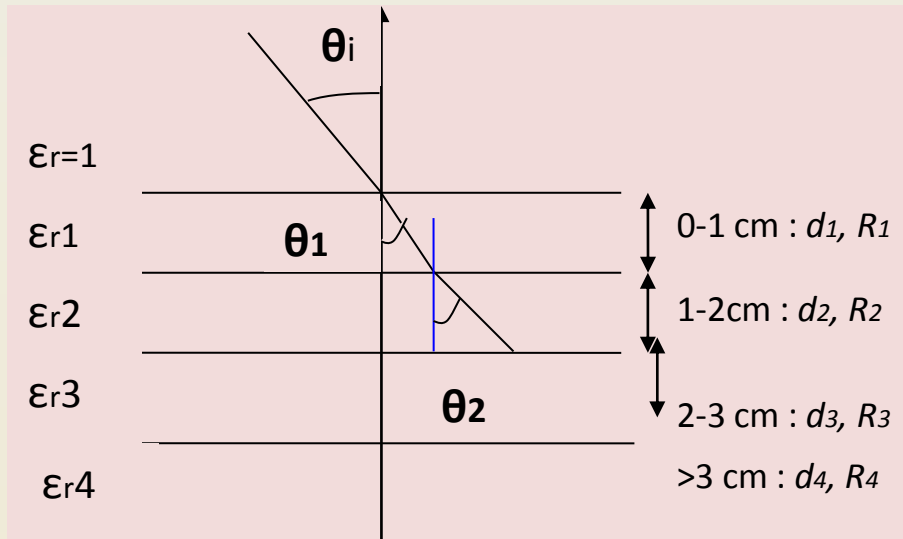


Simulated MM radar signals as a function of measured radar signals over agricultural fields, a) HH pol (b) VV pol

High discrepancy between measurements and simulations

- Effect of low scale structure
- Effect of volume scattering
- Effect of vertical moisture heterogeneity

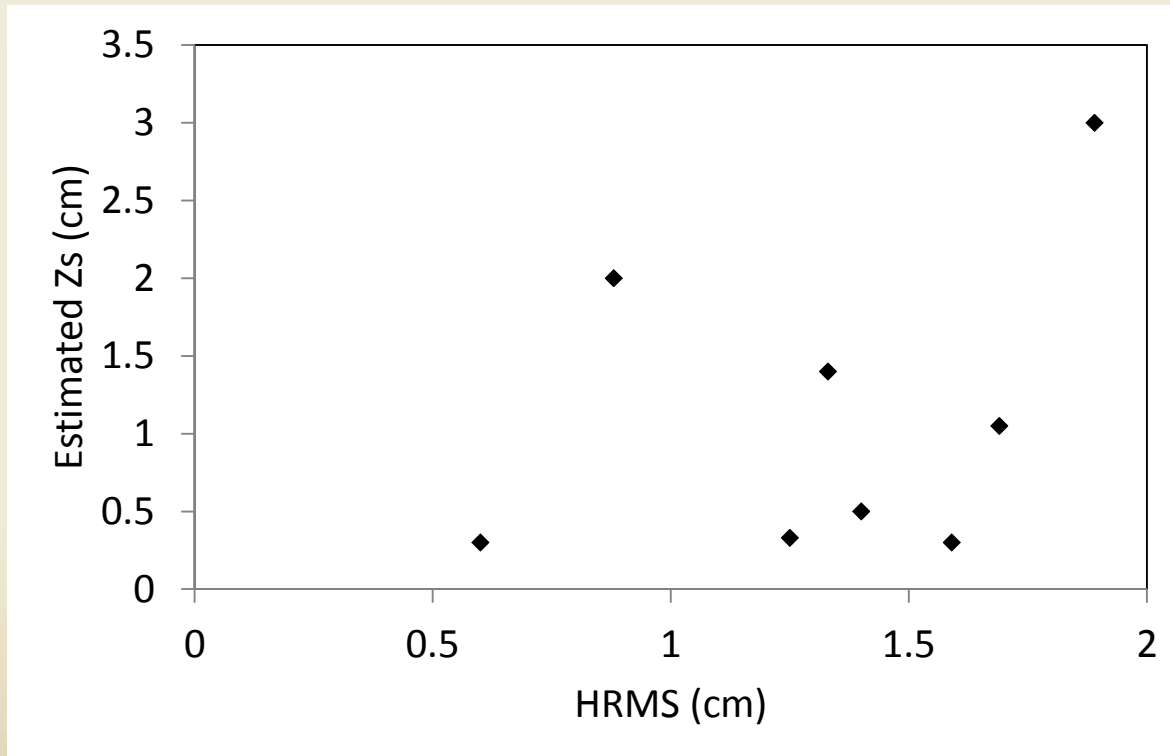
Results discussion, moisture heterogeneity



➤ Limited effect, lower than 1.5 dB

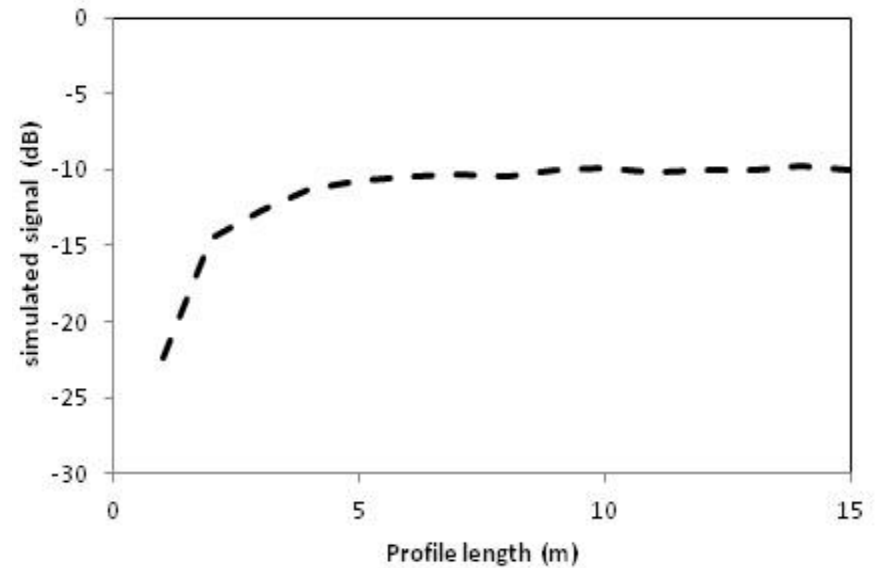
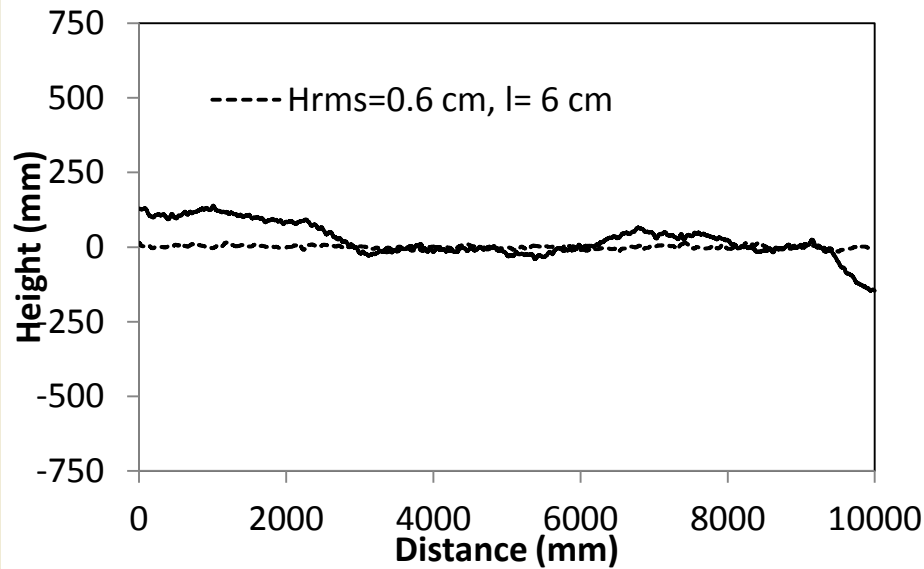
Retrieving of Zs low scale parameters for test fields

In the absence of ground truth measurements allowing the real value of low spatial frequency roughness to be determined, the proposed empirical model described before is used here, to retrieve the roughness parameter Z_s corresponding to eight test fields.



Estimated values of Z_s , plotted as a function of the in situ values of Hrms measured on eight test fields

Results discussion, errors due to profile length



➤ **Decreasing error with increasing of height profiles**

Conclusions

- Roughness is a key parameter in soil backscattering analysis
- Introduction of different parameters particularly useful for radar signal inversion (Z_s , Z_g etc)
- Principal roughness parameters to describe P-band radar signal over soil, H_{rms} for small scales and Z_s for low frequency scale
- Limited effect of small scale compared to low scale



Thank you for your attention!